

Mid-infrared Absorption Sensor for Measurements of CO and CO₂ in Propulsion Flows

R. Mitchell Spearrin¹, Jay B. Jeffries², and Ronald K. Hanson³
*High Temperature Gasdynamics Laboratory
 Department of Mechanical Engineering
 Stanford University, Stanford, CA 94305-3032*

An infrared laser absorption sensor was developed for gas temperature and carbon oxide (CO, CO₂) concentrations in high-enthalpy, hydrocarbon combustion flows. This diagnostic enables non-intrusive, *in situ* measurements in harsh environments produced by propulsion ground test facilities, utilizing tunable quantum cascade lasers capable of probing the fundamental mid-infrared absorption bands of CO and CO₂ in the 4 to 5 μm wavelength domain. A scanned-wavelength direct absorption technique was employed with two lasers, one dedicated to each species, free-space fiber-coupled using a bifurcated hollow-core fiber for remote light delivery on a single line of sight. The sensor was calibrated in a heated static cell, and field measurements were conducted in July, 2013 at the University of Virginia's direct-connect scramjet combustor for ethylene-air combustion. Measured quantities of carbon monoxide and carbon dioxide provide a basis for evaluating combustion completion or efficiency with temporal and spatial resolution in practical hydrocarbon-fueled engines.

Nomenclature

I_o	= incident spectral intensity [W/cm ² s ⁻¹]
I_t	= transmitted spectral intensity [W/cm ² s ⁻¹]
ν	= optical frequency [cm ⁻¹]
α	= absorbance
L	= path-length [cm]
S	= line-strength [cm ⁻² /atm]
E''	= lower-state energy [cm ⁻¹]
ν''	= lower-state vibrational quantum number
J''	= lower-state rotational quantum number
T	= temperature [K]
P	= total pressure [atm]
ϕ_ν	= line-shape function
χ	= gas mole fraction vector
x_{abs}	= mole fraction of the absorbing species
A	= integrated absorbance
ϕ	= C ₂ H ₄ -air equivalence ratio

¹ PhD Candidate, Department of Mechanical Engineering, AIAA Student Member.

² Senior Research Engineer, Department of Mechanical Engineering, AIAA Associate Fellow.

³ Professor, Department of Mechanical Engineering, AIAA Fellow.

I. Introduction

Advancements in air-breathing supersonic propulsion systems have led to the need for a new generation of diagnostic sensors to characterize the flow fields produced in these devices. While extensive analytical research has been dedicated to hydrogen-fueled supersonic combustors, systems that utilize hydrocarbon fuels have received more recent interest¹. Previous laser-based absorption diagnostics, typically probing water vapor, have proven valuable for assessing supersonic reacting gas systems²⁻⁵. Here we extend absorption sensing in scramjets to the other major hydrocarbon combustion species, CO and CO₂. This paper describes the development of a new quantum cascade laser absorption spectroscopy (QCLAS) sensor capable of providing non-intrusive, *in situ* measurements of temperature and carbon oxide species concentrations in high-speed hydrocarbon combustion flows. A wavelength-scanned direct absorption technique was used, targeting rovibrational carbon monoxide (CO) and carbon dioxide (CO₂) transitions, near 4854 nm and 4176 nm respectively, for a temperature range of 800 – 2400 K. The sensor was designed and developed at Stanford then utilized to simultaneously measure temperature and species mole fractions in ethylene-air combustion conditions at multiple planes of a direct-connect model scramjet combustor at the University of Virginia.

II. Spectroscopy and Methodology

Recent advances in tunable, room-temperature quantum cascade lasers enable access to the strong mid-infrared absorption bands of CO and CO₂ centered near 4.6 μm and 4.3 μm , respectively⁶. Wavelength selection within each band is primarily influenced by the isolation, strength, and temperature sensitivity of the discrete rovibrational lines that compose the bands, as well as laser availability.

Figure 1 shows the fundamental absorption bands for CO and CO₂ plotted as line-strengths at 2000 K⁷. At such combustion temperatures, we note the P-branch of CO₂ and the R-branch of CO interfere spectrally, and this overlapping domain was avoided for line selection. Two neighboring lines are chosen from the well-isolated P-branch of the fundamental carbon monoxide band near 2059.9 cm^{-1} and 2060.3 cm^{-1} to infer temperature and CO mole fraction. Carbon dioxide mole fraction is measured by probing a temperature-insensitive R-branch transition in the fundamental band near 2394.4 cm^{-1} . Relevant spectroscopic data is presented in Table 1 for the three selected transitions.

A wavelength-scanned direct absorption (DA) spectroscopy technique was used in this work to determine thermodynamic properties of interest from the measured absorption spectra. A brief discussion of the theoretical framework is outlined here. The Beer-Lambert law, given by equation 1, provides the fundamental relation governing narrow-band light absorption across a uniform gas medium.

$$\alpha_\nu = -\ln\left(\frac{I_\nu}{I_0}\right)_\nu = S_j(T)\phi_\nu(T, P, \chi)Px_{abs}L \quad (1)$$

Measured quantities of incident and transmitted light intensities define the spectral absorbance, α_ν , at wavelength ν , which is further related to the product of spectroscopic line parameters (S_j , ϕ_ν), the partial pressure of the absorbing species, and the optical path-length. By scanning the lasers in wavelength across each discrete transition j , the often complex dependence on the spectral line-shape can be eliminated, simplifying the measurement to an integrated absorbance area, A_j , which is only reliant on a single spectroscopic parameter, the line-strength, $S_j(T)$, as expressed in equation 2.

$$A_j = \int_{-\infty}^{\infty} \alpha_\nu d\nu = S_j(T)Px_{abs}L \quad (2)$$

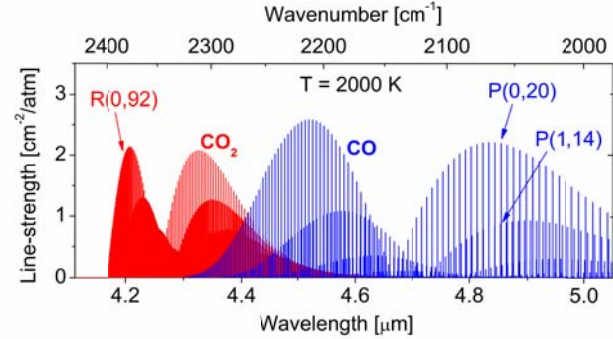


Fig. 1 Absorption line-strengths for CO and CO₂ from 4 – 5 μm ; T = 2000 K; transitions labeled as branch(ν'' , J'').

The ratio of integrated absorbance of two transitions further simplifies to a ratio of line-strengths, which is a function of temperature only. With the lower-state energy and line-strength at a reference temperature known for each transition (see Table 1), the simultaneous measure of two lines of a single species facilitates direct inference of gas temperature. Moreover, per equation 2, species mole fraction can be obtained from the absorption of each transition with concurrent knowledge of temperature, pressure, and path-length. Integrated absorbance areas for each line were determined by a Voigt line-shape fit to the measured absorbance profiles. Line-strength values for CO and CO₂ transitions are generally well-known due to the simple structure of the molecules, and taken here from the HITEMP 2010 database. These spectroscopic values were further validated at Stanford University in a heated static optical cell over a range of temperatures (500 – 800 K) and pressures (0.5 – 2 atm).

Table 1. Spectroscopic parameters of CO and CO₂ transitions used in the present sensor.

Line Assignment Branch(v'' , J'')	Species	Wavelength [nm]	Frequency [cm ⁻¹]	E'' [cm ⁻¹]	$S(296\text{ K})$ [cm ² /atm]
P(0,20)	CO	4855	2059.91	806.4	87.6×10^{-2}
P(1,14)	CO	4854	2060.33	2543.1	26.4×10^{-5}
R(0,92)	CO ₂	4176	2394.42	3329.0	73.9×10^{-6}

III. Experimental Setup

A. Optical Hardware

Figure 2 provides a graphical depiction of the optical configuration for the multi-species laser absorption sensor. For carbon monoxide, a distributed-feedback quantum cascade laser (ALPES) near 4860 nm provides a single-mode light source with ~10 mW output power. An external-cavity quantum cascade laser (Daylight Solutions) centered near 4250 nm provides single-mode light at 30 mW nominal output power for probing the carbon dioxide spectra. Each incident beam is free-space coupled into a 1.25 m bifurcated hollow-core fiber (OKSI, $d=300\ \mu\text{m}$), which combines the beams into a parallel and near co-linear path (300 μm core diameter separation) for pitching across the test medium. The fiber output is then re-collimated using a plano-convex silicon lens (f.l. = 40 mm) and transmitted through a wedged sapphire window. The combined beam, after passing through the test medium, is de-multiplexed using an anti-reflection coated CaF₂ beam splitter, and spectrally bandpass filtered (~50 nm) for each respective wavelength, followed by collection on two infrared thermo-electrically cooled photovoltaic detectors (Vigo PVI-4TE-5). The detectors have a bandwidth of 10 MHz, and 2 mm² detection area ($D^* \geq 3 \times 10^{11}\ \text{cmHz}^{1/2}\text{W}^{-1}$).

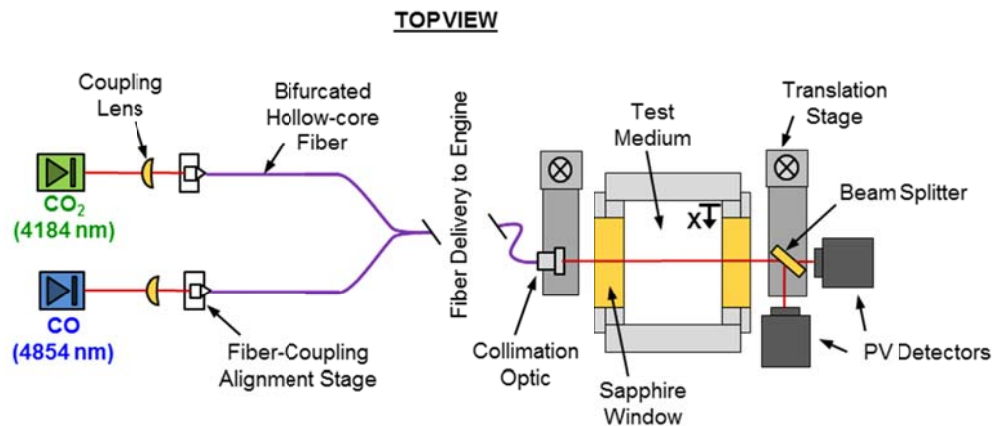


Fig. 2. Optical configuration for free-space fiber-coupling (left) and cross-section of scramjet combustor showing remote light delivery and collection. Flow direction is out of the page.

The CO DFB laser is centered at $2060.2\ \text{cm}^{-1}$ and scanned at 6 kHz (sawtooth) with an injection current amplitude of 80 mA, yielding a scan range of approximately $0.9\ \text{cm}^{-1}$ to capture both the P(0,20) and P(1,14) carbon monoxide transitions in a single laser scan. The external-cavity CO₂ QCL is centered at $2394.4\ \text{cm}^{-1}$, and piezo-electrically scanned at 100 Hz (sine wave), yielding a scan range of approximately $1\ \text{cm}^{-1}$. Prior to and between tests, the respective beams are redirected to a wavemeter (Bristol 621B) to confirm center wavelength. A

germanium Fabry-Pérot etalon, with a free-spectral range (FSR) of 0.016 cm^{-1} , facilitated data conversion from the time to wavelength domain.

B. Facility Interface

Initial field measurements using this sensor were carried out at the University of Virginia Supersonic Combustion Facility (UVaSCF)⁸. The direct-connect combustor was oriented vertically, with continuous air flow provided by a compressor and underground heater system. Air out of the heater had a total temperature of 1200 K, and was expanded by a nozzle to Mach 2 conditions prior to entering the combustor. Heated ethylene was injected through five ports located approximately 2.5 cm upstream of a cavity flame holder^{9,10}. Combustion products were exhausted by a pipe through the roof of the facility. The optical line-of-sight (LOS) was transverse to the injector with a path-length of 3.81 cm corresponding to the cross-sectional width of the combustor. Position of the optical LOS in the x-y plane was controlled by a set of high-precision translation stages (Zaber). Figure 3 illustrates a basic schematic of the combustor with representative optical lines of sight across a transverse measurement plane.

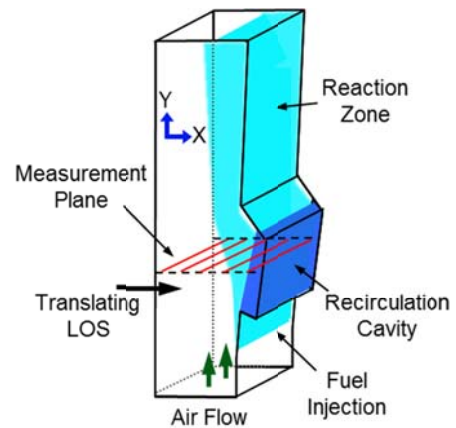


Fig. 3. UVaSCF supersonic combustor schematic; example optical lines of sight shown in red.

During combustor operation, a number of harsh thermo-mechanical phenomena were introduced to the ambient environment that required mitigation for successful sensor employment. To counter mechanical vibrations and acoustic perturbations, the lasers were mounted to a honeycomb vibration-dampening breadboard. Due to radiation of the combustor, the photovoltaic detectors were mounted to water-cooled plates to prevent saturation or damage due to overheating. Heating in the room also led to elevated levels of water vapor in the humid ambient air, which could spectrally interfere with the absorption measurements and condense on cooled optical equipment. A nitrogen purge of the optical breadboard was constructed to remove this water vapor. The N_2 purge was extended to the hollow-core fiber and optical detection components as well to encompass the entire optical path of each laser output.

IV. Sensor Demonstration

The present mid-infrared sensor aimed to measure gas temperature, carbon monoxide, and carbon dioxide simultaneously with both temporal and spatial resolution in the harsh combustion environment. Raw data quality can be examined by inspection of the laser scans, exhibited in figures 4a and 5a, for CO and CO_2 respectively. Transmitted laser light intensity, in detected volts, is shown along with the baseline intensity, which was captured after flame extinction. For the DFB QCL dedicated to CO measurements, the sawtooth scan (see fig. 4a) was deliberately set to go below the threshold current of the laser for a short time, during which thermal emission could

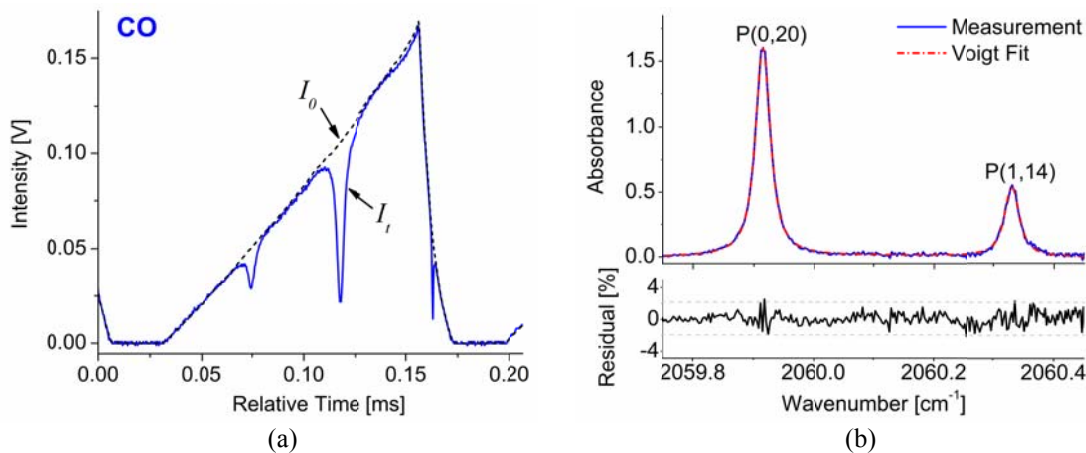


Fig. 4. Measured carbon monoxide absorption from a single laser scan (6 kHz) shown as (a) raw voltage signals versus time and (b) absorbance versus wavenumber; $T = 1725 \text{ K}$, $P = 0.71 \text{ atm}$, $L = 3.81 \text{ cm}$, $X_{\text{CO}} = 0.057$; $\phi \approx 0.15$, measurement location in combustor cavity.

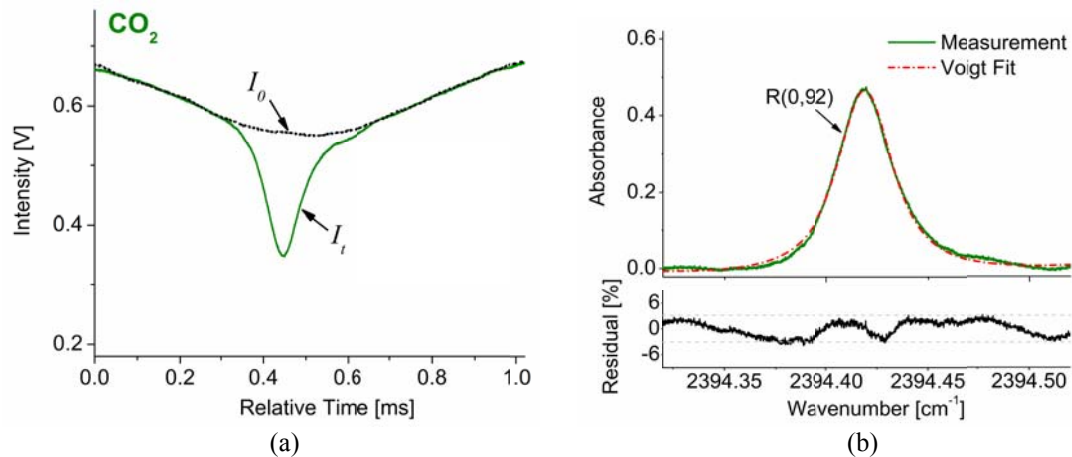


Fig. 5. Measured carbon dioxide absorption from a single laser scan (100 Hz) shown as (a) raw voltage signals versus time and (b) absorbance versus wavenumber; $T = 1725$ K, $P = 0.71$ atm, $L = 3.81$ cm, $X_{\text{CO}_2} = 0.062$; $\phi \approx 0.15$, measurement location in combustor cavity (same as figure 4).

be measured and subtracted from the adjacent signal. For the ECQCL dedicated to CO_2 , the piezo-scan simply tunes a mechanical grating such that laser output intensity is nearly constant across the laser scan (see fig. 5a). Therefore, to account for thermal emission, a beam chopper (~ 12.5 Hz) was mounted at the output of the ECQCL to intermittently block the laser after every eight scans for a period of ~ 5 ms wherein thermal emission was measured and subtracted in a similar manner as described above. Due to the temperature- and wavelength-dependent transmission of the sapphire windows, the baseline, which was measured at a lower temperature after combustion ceased, was scaled to match the non-absorbing regions of the transmitted intensity scan. Figures 4b and 5b show the conversion of the raw intensity signals to absorbance and transposed to the wavenumber domain, from which the Voigt line-shape function could be fit to each transition to yield the integrated absorbance areas.

Since line-strengths are well known for the selected transitions, the quality of the baseline and Voigt fits typically limit measurement uncertainty for scanned-wavelength direct absorption techniques in harsh environments. With such large absorbance in this application, these uncertainties are small in most measurement locations, and can be partly quantified by inspection of the residual to the Voigt fit and corresponding signal-to-noise ratio (SNR). For CO detection, both lines as depicted in figure 4b exhibit $\text{SNR} > 30$ with no systematic baseline error ($< 1\%$). The SNR degrades nearly linearly with mole fraction, yielding a CO detection limit of ~ 1000 ppm in this work. The carbon dioxide measurements are more prone to baseline distortion resulting from random fluctuations in laser output power ($\sim 2\%$) due to sensitivity of the ECQCL to vibrations, though a similar detection limit of ~ 1200 ppm was achieved.

A. Time-Resolved Measurements

The time resolution of each species measurement is equivalent to the scan rate of each QCL that comprises the sensor: 6 kHz for CO, and 100 Hz for CO_2 . Such bandwidths, especially for the faster CO DFB laser, can provide valuable time-resolved information about flow field properties. Figure 6 shows the integrated absorbance areas for each of the two CO transitions, measured at a fixed x-y location in the combustor cavity during ethylene-air combustion conditions ($\phi = 0.15$). Each data point represents the result from a single laser scan as described above. The integrated areas are observed to vary dramatically ($> 25\%$) scan to scan. The positively correlated trends over time between the P(0,20) and P(1,14) areas supports the physical nature of this fluctuation. We further note that the physical oscillations in temperature at a fixed position in the combustor are

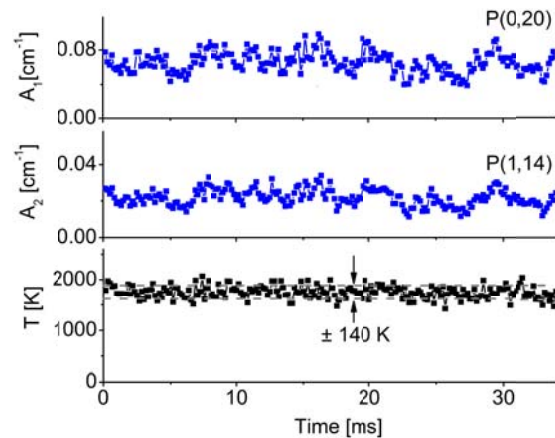


Fig. 6. Representative time-resolved CO absorbance areas and temperature at a fixed x-y position in the combustor cavity; ethylene-air, $\phi = 0.15$.

much smaller ($< 10\%$) than the fluctuations in mole fraction, which scales linearly with absorbance area. For both temperature and species concentrations, these physical variations are much greater than measurement uncertainty. This time-resolved data provides a basis to evaluate combustion stability and gas dynamic events.

B. Spatially-Resolved Measurements

In addition to high bandwidth measurements, the current experimental setup facilitates carbon oxide sensing with two-dimensional spatial resolution. The translation stages can position the optical line of sight along a plane transverse to the flow streamlines (x-axis) as illustrated in figure 3 and at multiple planes along the flow direction (y-axis). Spatially-resolved species measurements in the combustor facilitate assessment of flame structure and combustion progress. Figure 7 provides example data of CO and CO₂ mole fraction measured across a transverse plane in the model scramjet combustor at an axial location in the flame holding cavity (see fig. 3). The two plots represent a snapshot of the same measurement plane under different fuel to air mass flow ratios ($\phi_a = 0.15$ and $\phi_b = 0.21$). All data points are time-averaged over approximately one second, and the error bars represent the standard deviation (physical oscillations) of the mole fractions over this time interval. Water concentration, which was measured independently at the same test conditions, is also shown for reference¹¹.

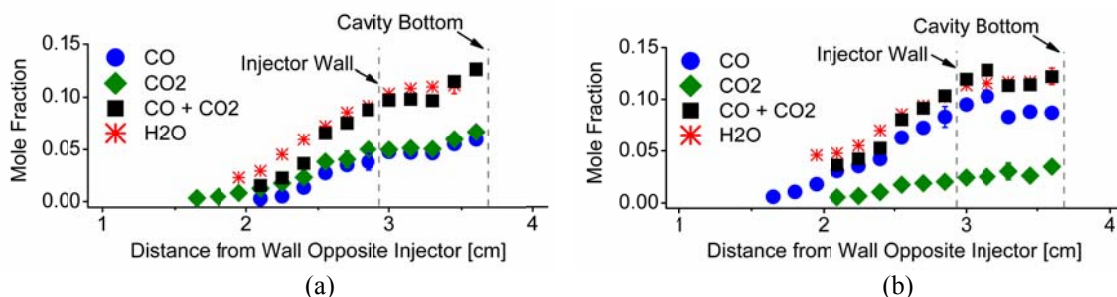


Fig. 7. Carbon oxide mole fraction measurements across the cavity plane for ethylene-air combustion at (a) $\phi = 0.15$ and (b) $\phi = 0.21$. X_{H_2O} also shown.

Though combustor analysis is reserved for another publication, these example data highlight the value of this *in situ* carbon oxide sensor, and a few observations deserve mention. We observe that conditions in the cavity appear near stoichiometric or rich while carbon oxides become quickly diluted once entering the free stream, both trends that would be expected. Comparing the aggregate carbon oxide concentration with values of independently measured H₂O, we find excellent consistency with C₂H₄ atom balance ($X_{CO} + X_{CO_2} = X_{H_2O}$) for both conditions, even while relative carbon oxide levels vary considerably between equivalence ratios. These observations provide physical validation to the measurements, but also point to the strength and sensitivity of the diagnostic approach. At $\phi = 0.15$, peak CO and CO₂ mole fractions are both near 6%, while at $\phi = 0.21$, the peak values are approximately 10% and 3%, respectively. Similarly comparing the H₂O measurements across equivalence ratios, we note that mole fractions peak around 12% (a near stoichiometric level) for both conditions, suggesting that the CO and CO₂ measurements are each a more sensitive measure of combustion progress for ethylene-air. Moreover, due to the inverse relationship of CO and CO₂ with combustion progress, the combined measurement (CO:CO₂ ratio) yields even greater sensitivity. These observations reinforce the strength of the two-species carbon oxide sensing strategy for assessing hydrocarbon combustion.

V. Conclusion

A mid-infrared quantum cascade laser absorption sensor was developed for simultaneous measurements of carbon monoxide, carbon dioxide, and gas temperature in supersonic propulsion flows. Two QCLs comprised the sensor, coupled with a bifurcated hollow-core fiber for remote light delivery. The sensor was successfully demonstrated at the University of Virginia's direct-connect scramjet combustor facility for time-resolved detection (up to 6 kHz) at multiple fuel-air flow ratios, with detection limits of ~ 1000 ppm for each species. Spatially-resolved measurements across the combustor highlighted the sensitivity of a combined CO/CO₂ sensor to hydrocarbon combustion progress. To the authors' knowledge, these measurements represent the first quantitative, *in situ* detection of CO and CO₂ in a scramjet combustor.

Acknowledgments

This work was sponsored by the National Center for Hypersonic Combined Cycle Propulsion (NCHCCP), grant FA 9550-09-1-0611, with technical monitors Chiping Li (AFOSR) and Rick Gaffney (NASA). The authors would also like to thank Bob Rockwell, Brian Rice, and Roger Reynolds of the University of Virginia for their assistance in operating the UVaSCF facility.

References

- ¹Tishkoff, J. M., Drummond, J. P., Edwards, T., and Nejad, A. S., "Future directions of supersonic combustion research - Air Force / NASA workshop on supersonic combustion," *35th Aerospace Sciences Meeting and Exhibit*, Reno, NV: 1997.
- ²Rieker, G., Jeffries, J., Hanson, R., Mathur, T., Gruber, M., and Carter, C., "Diode laser-based detection of combustor instabilities with application to a scramjet engine," *Proceedings of the Combustion Institute*, vol. 32, 2009, pp. 831–838.
- ³Liu, J. T. C., Rieker, G. B., Jeffries, J. B., Gruber, M. R., Carter, C. D., Mathur, T., and Hanson, R. K., "Near-infrared diode laser absorption diagnostic for temperature and water vapor in a scramjet combustor," *Applied Optics*, vol. 44, Nov. 2005, p. 6701.
- ⁴Li, F., Yu, X., Gu, H., Li, Z., Zhao, Y., Ma, L., Chen, L., and Chang, X., "Simultaneous measurements of multiple flow parameters for scramjet characterization using tunable diode-laser sensors," *Applied Optics*, vol. 50, Dec. 2011, pp. 6697–707.
- ⁵Griffiths, A., and Houwing, A., "Diode laser absorption spectroscopy of water vapor in a scramjet combustor," *Applied Optics*, vol. 44, 2005, pp. 6653–6659.
- ⁶Namjou, K., Cai, S., Whittaker, E. A., Faist, J., Gmachl, C., Capasso, F., Sivco, D. L., and Cho, A. Y., "Sensitive absorption spectroscopy with a room-temperature distributed-feedback quantum-cascade laser," *Optics Letters*, vol. 23, Feb. 1998, p. 219.
- ⁷Rothman, L. S., Gordon, I. E., Barber, R. J., Dothe, H., Gamache, R. R., Goldman, a., Perevalov, V. I., Tashkun, S. a., and Tennyson, J., "HITEMP, the high-temperature molecular spectroscopic database," *Journal of Quantitative Spectroscopy and Radiative Transfer*, vol. 111, Oct. 2010, pp. 2139–2150.
- ⁸McDaniel, J. C., Goyne, C. P., Bryner, E. B., Le, D. B., T, S. C., and Krauss, R. H., "Dual-mode scramjet operation at a mach 5 flight enthalpy in a clean air test facility," *AIP Conference Proceedings*, AIP, 2005, pp. 1277–1282.
- ⁹Gruber, M., and Donbar, J., "Mixing and combustion studies using cavity-based flameholders in a supersonic flow," *Journal of Propulsion and Power*, vol. 20, 2004, pp. 769–778.
- ¹⁰Ben-Yakar, A., and Hanson, R., "Cavity flame-holders for ignition and flame stabilization in scramjets: an overview," *Journal of Propulsion and Power*, vol. 17, 2001, pp. 869–877.
- ¹¹Goldenstein, C. S., Schultz, I. A., Spearrin, R. M., Jeffries, J. B., and Hanson, R. K., "Scanned-wavelength-modulation spectroscopy near 2.5 μm for H_2O and temperature in a hydrocarbon-fueled scramjet combustor," submitted to *Applied Physics B*, 2013.